RSSI, Vol. 07, N°. 02, December 2018, 10-17

Revue des Sciences et Sciences de l'ingénieur
Journal of sciences and engineering sciences
ISSN 2170-0737/EISSN: 2600-7029
https://www.asjp.cerist.dz/en/PresentationRevue/303

Study and Mitigation of AC Corrosion on Pipelines Nearby the HV Power Lines

***Fatiha BABAGAYOU, Boubakeur ZEGNINI, Tahar SEGHIER**

Laboratory for the Study and Development of Semiconductors and Dielectric Materials, Amar Telidji University Laghouat, Algeria b.**zegnini**@lagh-univ.dz

Article history
Submitted date: 2017-07-31
Acceptance date: 2018-10-07
DOI: 10.34118/rssi.v7i2.1714

Abstract

HV power lines induce an AC, this latter causes corrosion damages on adjacent metallic structures. Therefore, the petroleum companies do confront serious corrosion problems of the underground pipelines nearby HV power lines, even where pipelines are protected by an insulation coating and the cathodic protection (CP). Therefore, we conducted a study, which we can summarise in three points. To begin with, we did a theoretical analysis to explain the fundamental mechanisms of AC corrosion. Afterwards, we did an experimental investigation on a laboratory model, to realise electrochemical tests on a pipeline steel sample. Then, as we found that the AC corrosion numerical simulation study is minimal in the electrochemical and the electrical fields, we did further numerical simulation studies. This latter contains the study of the electrochemical reactions of the corrosion phenomena such as anodic process and cathodic process; i.e. the iron oxidation and the reduction of both the oxygen and the hydrogen. We have also simulated the CP, the AC corrosion and the pipeline sample deformation. At last, to solve this problem, we developed a monitoring and correction program for optimising the AC corrosion. In this article, we represented the obtained experimental and numerical simulation results. In addition, we want also to mention the original and personal added values in both studies.
Key-words: *induced AC; AC corrosion; immunity; reference potential; cathodic protection.*

Résumé

Les lignes aériennes de transport d'énergie électrique de haute tension (HT), partagent parfois le même chemin que les pipelines souterrains. Ces derniers sont protégés de la corrosion par un revêtement isolant et une protection cathodique (PC), mais, les lignes de HT voisines induisent un courant alternatif (CA), qui provoque de graves dommages de corrosion de la structure métallique des pipelines, c'est le phénomène de la corrosion par CA. Dans notre étude, nous avons réalisé, au laboratoire, des tests et des essais électrochimiques sur des échantillons de terrain, puis, nous avons effectué des modélisations et simulations numériques des réactions électrochimiques ayant lieu dans la corrosion, tels que les processus anodiques et cathodiques, c.à.d, l'oxydation du Fer et la réduction de l'oxygène et l'hydrogène. Nous avons, également simulé la PC, la corrosion par CA et la déformation du fer de l'échantillon de pipeline. Finalement, pour remédier au problème de la corrosion par CA, nous avons développé un programme de surveillance et de correction automatique de la PC, afin d'optimiser les risques de cette dernière. La nouveauté dans notre travail réside dans notre modélisation du phénomène et nos résultats des tests expérimentaux et ceux des simulations numériques, qui ont été en bon accord ainsi que le développement d'un programme de surveillance et de remédiation automatique à la corrosion par CA.

Mots-clés: *CA induits; corrosion; immunité; potentiel de référence; protection cathodique.*

1. Introduction

The overhead high voltage power transmission lines influence buried pipelines by inducing AC currents; consequently, it causes the perturbation of the cathodic protection (CP) leading to severe corrosion damages.

The AC corrosion has become a problem only in the last thirty years, after the growth in the number of interference sources, such as the traction systems and AC-powered electrical transmission lines that share the same path with buried pipelines for long distance, because of the space limitation imposed by private or governmental entities [1; 2]. In recent decades, the insulation capacity improvement of the cathodically protected pipe coating has aggravated the AC corrosion problem: the passage from the usage of bitumen and particularly polyethylene and polypropylene extruded, allowed the increase of the electrical resistivity coating and minimised the size and the defects number; this was an advantage because it reduced the delivered CP current but caused a high interfering AC densities at the defects area. Many authors considered this as one of the main reasons for the increase in the corrosion cases number attributable to AC interference [2-4], and many researchers have carried substantial studies in this field such as A. Brenna et al. [1], L.V. Nielsen [3], D. Qingmiao et al. [5] and The International Institute NACE.

To remedy this problem, companies had to replace defective sections, which is very costly.

To solve this problem, we simulated this phenomenon and we conducted investigations that can be summed up in three points. First, we conducted a theoretical research to explain the basic electrical and electrochemical mechanisms of the AC corrosion. Second, we carried out electrochemical tests on a laboratory model by using a sample of the pipeline steel type API 5L X52, which is used in Algeria. For realising our experimental investigation, we used an advanced electrochemical workstation potentiostat and galvanostat EC-LAB VSP300, it allowed us to simplify the studied phenomenon model, and it provided all our measurements, we used a test cell containing a pipeline's sample, and a solution to simulate soil. In the first time, the test cell was subjected to free potential measurements, which means without both CP and AC, then, we applied a DC as CP to the sample. The measurements of the reference potential E_{off} close to the iron sample allowed us to select an appropriate CP; then we added an AC in order to simulate the induced current. The results illustrated that the induced AC causes the sample corrosion even in cathodic protection condition; this results are consistent with the theoretical study. The third point we did, was a numerical simulation study to digitally represent the test cell, the CP phenomenon and the AC corrosion, then we suggest an efficient solution for minimising its impact on pipelines. For this numerical simulation, we used the COMSOL Multiphysics software [6], we introduced all parameters of both of the iron sample and simulating the soil solution. We measured the E_{off}, we selected the appropriate CP, which brings the immunity state, and then we added AC for simulating the induced current. In this last case, the measured results gave an E_{off} exceeding the immunity zone regarding standards [7], a strong iron oxidation, a significant oxygen reduction, a high hydrogen liberation and a clear sample deformation. All these results mean that corrosion took place in our pipeline sample, which was cathodically protected, when it was subjected to an induced AC. These numerical results validate the experimental study results. Finally, we have set up a monitoring and correction program to bring the E_{off}, in the AC presence, in the immunity corrosion zone according to standards. Our monitoring program was able to minimize the electrochemical process reactions, and it prevented the sample's deformation because it can automatically test, calculate and choose for each case a safety CP.

2. Theoretical Study of Corrosion by AC

We conducted a conscientious theoretical research that shows the main AC corrosion mechanism of the API type pipelines and illustrates multiple points such as the different AC interference types [1], the AC corrosion [8], the corrosion electrochemical explanation [9], the standards, the Pourbaix corrosion diagram and immunity areas [1; 2; 7], the cathodic protection [1; 9], the measurement corrosion parameters [1] and the principal AC corrosion mechanism models [8].

3. Experimental study

In order to do the experimental investigation, we have used an advanced electrochemical workstation potentiostat and galvanostat EC-LAB VSP300. It allowed us to simplify the model of the studied phenomenon, and it provided all of our measurements. We conducted the electrochemical tests on the laboratory model, we used a test cell containing an Iron sample of pipeline type API 5L X52, and a solution to simulate the soil.

Below the electrochemical process reactions [10]: Anodic Process eq. (1) and Cathodic Process: eq. (2), eq. (3), eq. (4).

$$Fe \rightarrow Fe^{2+} + 2e^{-} \quad (1)$$

$$4e^{-} + O_2 + 2H_2O \rightarrow 4OH^{-} \quad (2)$$

$$2e^{-} + 2H_2O \rightarrow 2OH^{-} + H_2 \quad (3)$$

$$2e^{-} + 2H^{+} \rightarrow H_2 \quad (4)$$

3.1 Material and methods (Electrode, Electrolyte and Measuring device)

The working electrode was API 5L X52 steel with the chemical composition: 0.31% Manganese, 1.35% Carbon, 0.030% Sulphur and 0.030% Phosphor as shown in Fig. 1a. The electrode is a metallic conductor, thus its potential relation [1; 10]:

$$\Phi_S = E_{CP} + E_{AC} = E_{CP} + A.\sin(2\pi.f.t) \quad (5)$$

where E_{CP} is the applied potential of CP, E_{AC} is the AC potential, A is the AC potential amplitude and f is the frequency (50 Hz).

According to the literature, Electromagnetic Coupling Interference (Inductive) is identical to the secondary induced current of a transformer, ie it is an alternating current whose expression is sinusoidal.The electrolyte, as shown by Fig. 1b, is composed by a soil-simulating solution [1]: 200 mg/L chlorides (0.33 g/L of *NaCl*) and 500 mg/L sulphate ions (0.74 g/L of Na_2SO_4). It was prepared from distilled water and analytical grade reagent for the electrochemical tests.

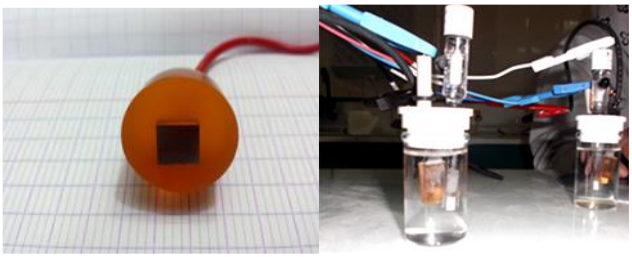

Fig. 1. (a) Sample – Iron (API 5L X52) (b) Cell – Sample, Electrolyte (*NaCl*, Na_2SO_4), Reference electrode, Counter electrode.

The Measuring device is the potentiostat and galvanostat EC-LAB VSP300 for applying DC (CP) and AC simultaneously to the sample (Fig. 2).

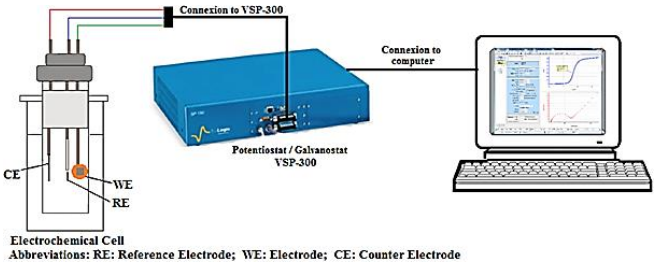

Fig. 2 shows the schematic diagram of the experimental setup of AC corrosion of pipeline steel.

Fig. 2. Schematic diagram of experimental setup

3.2 Steps of the experimental tests

We have followed the below steps for carrying out the experimental tests:

First step, we used the free potential procedure to highlight the corrosion process in the absence of PC and AC.

Second step, we applied the linear polarization method to find the area where the sample did not oxidize, which we called the immunity zone.

Third step, we selected the appropriate CP, where the E_{off} was in the immunity zone, in the absence of AC.

Final step, we applied a variable value of the induced current (AC) and we measured the E_{off}, to underscore the restriction zone overshooting.

4. Numerical Modelling

We have done a simulation study in order to digitally represent the CP phenomenon, AC corrosion and optimise AC corrosion behaviour by changing the CP in the case of AC interferences. We developed a monitoring program that returns the process status to the immunity zone by referring to Pourbaix diagram and CP Hosokawa criteria [2; 7; 19]. The immunity zone is -1150 mV < E_{off} < -850 mV, where E_{off} is the reference potential sensed by the reference electrode. Numerical simulations are based on:

4.1 The Model Geometry

This simulation required the parameters initial value configuration [6] (Electrolyte conductivity, Diffusion coefficient of *Fe*, O_2 and H_2, Tafel slope iron oxidation, …), and the electrochemical composition of iron API 5LX52 pipeline definition (Fig. 3) in "Material Overview" section [6].

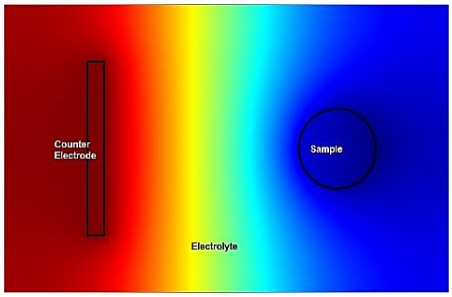

Fig. 3. The Model Geometry: Sample, Counter Electrode and Electrolyte.

4.2 The parameterisation of current distribution in cell

The electrode is a metallic conductor; thus its current-voltage relation is obeyed to Ohm's law [11]:

$$i_s = -\sigma_s \nabla \Phi_s \qquad with \qquad \nabla . i_s = Q_s \tag{6}$$

where i_s is the current density (A/m^2) in the electrode, σ_s is the conductivity (S/m), Φ_s is the electric potential (V), and Q_s is the general current source term (A/m^3).

The electric potential Φ_s is defined as [1; 10]:

$$\Phi_s = E_{CP} + E_{AC} = E_{CP} + A.\sin(2\pi . f . t) \tag{7}$$

where E_{CP} is the applied potential of CP, E_{AC} is the AC potential, *A* is the amplitude, and *f* is the frequency (50 Hz).

The electrolyte, which is an ionic conductor, the net current density can be described, using the sum all ions fluxes:

$$i_l = -\sigma_l \nabla \Phi_l \qquad with \qquad \nabla . i_l = Q_l \tag{8}$$

where i_l is the current density (A/m^2) in the electrolyte, Φ_l is the electrolyte potential (V)

The difference between the actual potential difference and the equilibrium potential difference is the activation over-potential η (Electrode-Electrolyte-Interface) [7; 11; 12]:

$$\eta = Q_s - Q_l - E_{eq} \tag{9}$$

where E_{eq} is the equilibrium potential, and it is given by Nernst's equation [1].

4.3 The transport of chemical species

In order to configure the concentration and the chemical species movement (*Fe*, O_2, H_2) [12], the driving forces for transport can be diffused by Fick´s law, convection when coupled to a flow field, and migration, when coupled to an electric field.

$$(\sigma c_i / \sigma t) + \nabla(-D_i \nabla c_i) + u \cdot \nabla c_i = R_i, \quad (10)$$

where for the species *i*, c_i is the concentration (mol/m^3), D_i is the diffusion coefficient (m^2/s), *u* is the velocity vector (m/s), and R_i is the reaction rate expression (mol/(m^3.s)) [11].

The flux vector *N* (mol/(m^2.s)) is associated with the mass balance equation above and used in boundary conditions and flux computations. For the case where the diffusion and convection are the only transport mechanisms, the flux vector is defined as [11]:

$$N_i = -D_i \nabla c_i + u c_i \quad (11)$$

4.4 The math ODE and DAO Module

We used this module in COMSOL multi-physics to support the monitoring program to bring the situation to the immunity state, below the simplified algorithm used.

program beginning
  read E_{eq}
  Lib1: read E_{AC}, E_{CP}, E_{off}
  if (E_{off}>-1.15V and E_{off}<-0.85V) goto Lib1
    Calculate a new E_{CP} and other parameters
    Apply the new E_{CP} and other parameters
  endif
  goto Lib1
end of program

4.5 The sample deformation by corrosion

From the Cathodic Tafel expression to describe the reaction kinetics and anodic Tafel expression for the anodic electrode reaction current density [12]:

$$i_{cat} = -i_{0,cat}.10^{\frac{\eta}{A_{cat}}}, \qquad i_{tafel} = -i_{0,an}.10^{\frac{\eta}{A_{an}}}$$

and $$i_{an} = \frac{\left(i_{tafel}.i_{\lim}\right)}{\left(i_{tafel} + i_{\lim}\right)} \quad (12)$$

where i_0 is the exchange current density, η is the over-potential of the reaction, A_{an} and A_{cat} are the Tafel slope, and i_{lim} is limiting current density. The iron metal dissolution makes the electrode boundary moving, with a velocity in the normal direction, v (m/s), according to:

$$v = \left(\frac{i_{an}}{2F}\right)\left(\frac{M}{\rho}\right) \quad (13)$$

where *M* is average molar mass, ρ is the iron density, *F* is Faraday constant (C/mol).

4.6 The Boundary Condition

The boundary condition applied to the insulating surface is the potential gradient perpendicular to the surface and is equal to zero. The potential of the anode is fixed. The potential of the structure is assumed unknown and described on every point k by the equation:

$$U_k = V_k - E_{ok} - \eta_k(-\sigma \frac{\partial U_k}{\partial n}) \quad (14)$$

where U_k is the potential in the soil adjacent to the point considered, V_k the potential of the metallic part of the structure, E_{ok} the Nernst potential of the metal-soil system,

and $\eta_k(-\sigma \frac{\partial U_k}{\partial n})$ the polarization voltage resulting from

electrochemical reactions (mass and charge transport).

5. Results and discussion

5.1 Free potential in the absence of CP and AC

This test aims to verify that, in the absence of CP, the sample undergoes oxidation. The EC-Lab analysis software shows that without the CP, The potential decreases and stabilises at -500 mV, the device also gives us E_{corr} = -500 mV and sample oxidation took place.

5.2 The good immunity area and the adequate CP

We applied the Linear Polarization analysis method Log i (E_{off})) [10] on two different pipeline samples. This technique allows us to sweep in the same curve for both of the reduction area and the oxidation zone. In the reduction area of iron samples, i.e. the no oxidation part; we can choose the immunity zone between -960 mV and -670 mV. Regarding our results, we can also choose the adequate CP in the middle of the restraining zone: CP ≈ -800 mV. That means for CP= -800 mV and -960 mV < E_{off} < -670 mV, the sample does not undergo any corrosion; it is in the immunity zone. These tests results are consistent with the standards.

1.1 Application of an AC in the CP presence

By applying the ACV technique (AC voltammetry VSP-300) [10] and E_{off} potential monitoring, for several periods and different AC values, we had the following results.

For CP = -800 mV and AC = 100 mV, the sample was in reduction state, and E_{off} was in immunity area as shown in Fig. 4.

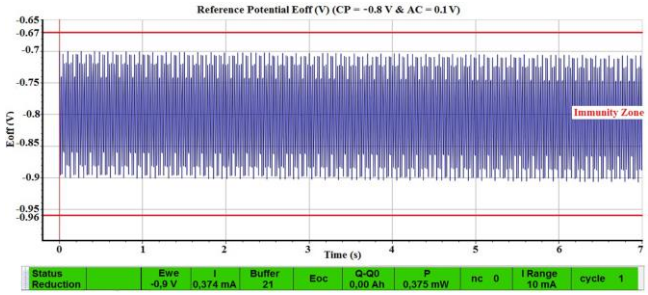

Fig. 4. Potential E_{off} for CP= -800 mV and AC=100 mV

For CP = -800 mV and AC = 400 mV, the sample was in oxidation state and E_{off} exceeded the immunity area as shown in Fig.5 .

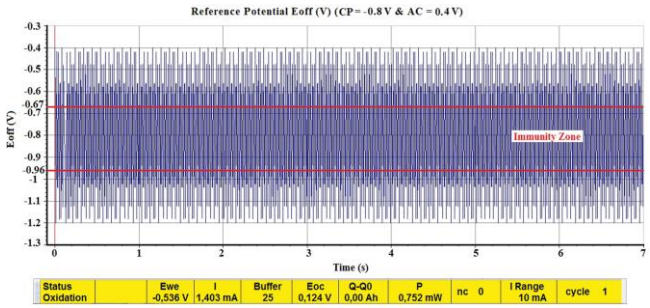

Fig. 5. Potential E_{off} for CP= -800 mV and AC=400 mV

We can say that the use of the potentiostat and galvanostat EC-LAB VSP-300 gave us the opportunity to facilitate the studies on AC corrosion by the application of the two currents DC and AC at the same time on the sample, and it allowed us to present many applications and analytical techniques.

1.2 The potential E_{off} in the presence of CP

Fig. 6 shows that the potential E_{off} in the CP and AC presence (Amplitude A=100 mV) did not exceed the immunity zone, in this case, we did not need to modify the CP.

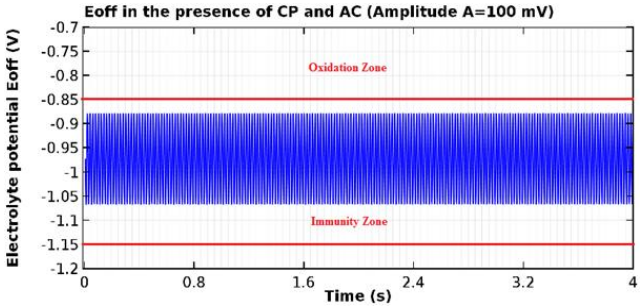

Fig. 6. E_{off} in the presence of CP & AC (Amplitude A=100 mV)

Fig. 7 (Amplitude A=500 mV) illustrate that E_{off} exceeded the immunity area; therefore there is a significant corrosion risk. Then for the same values of AC and by introducing the immunity program resolution (Paragraph 4.4), we were able to bring the E_{off} to the immunity zone. Secondly, we measured the different species concentration of the electrochemical process.

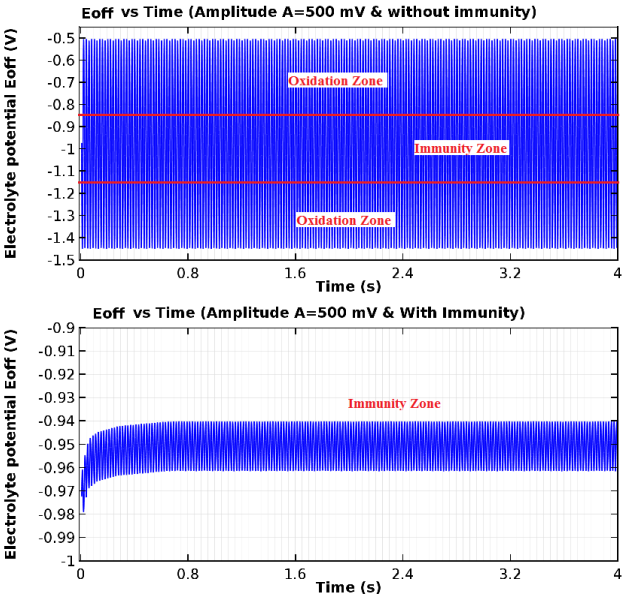

Fig. 7. E_{off} in the presence of CP and AC (Amplitude A=500 mV)

1.3 The Concentration of iron ions Fe^{2+}, Oxygen O_2 and Hydrogen H_2 near the sample

Fig. 8(a) shows that the Iron ions Fe^{2+} concentration was on the increase, thus demonstrated that a reaction of iron oxidation eq. (1) took place, indicating a corrosion state. After the implementation of the immunity program, this concentration has decreased. Fig. 8(b) illustrates the significant Oxygen O_2 concentration decrease, so, we had a strong reduction reaction of Oxygen eq. (2), implying that it was a case of a strong corrosion. After the implementation of the immunity program, this concentration has increased. Fig. 8(c) shows that the Hydrogen H_2 concentration was on the increase; it demonstrated that it was a reduction reaction of H_2O eq. (3) or H^+ eq. (4), indicating that a significant corrosion took place. After the immunity program implementation, this concentration has decreased.

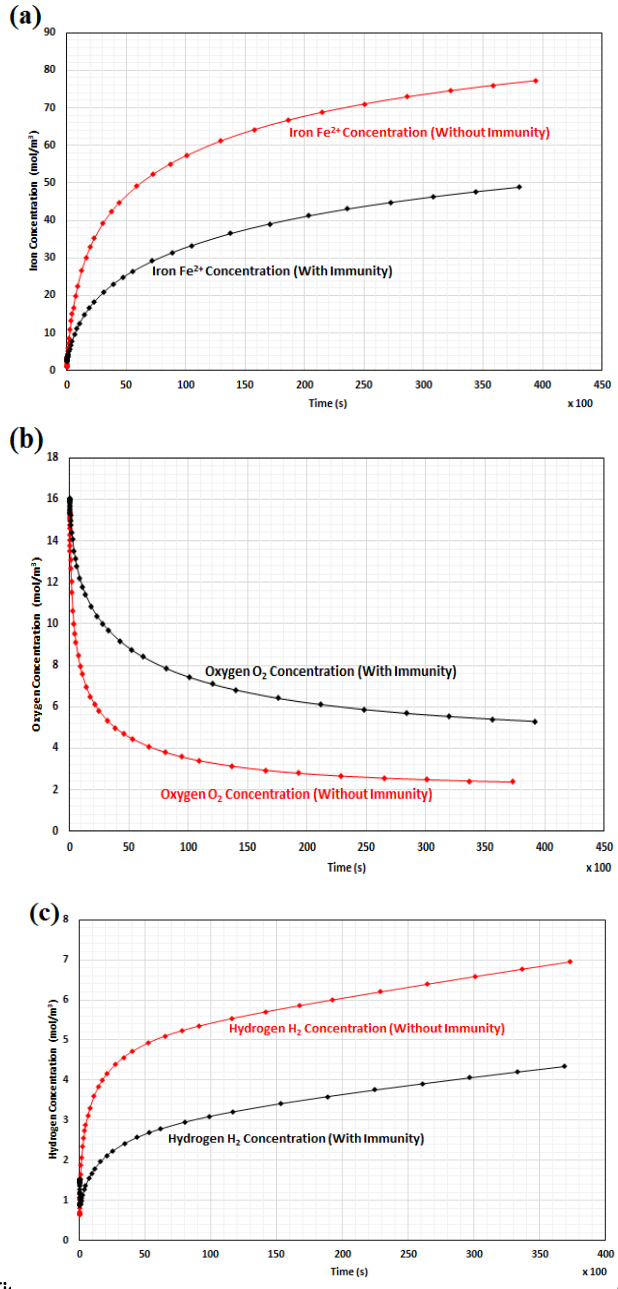

Fig. 8. Concentration of (a) Iron ions Fe^{2+}; (b) Oxygen O_2; (c) Hydrogen H_2

1.4 The Sample Deformation under CP and AC

Finally, we studied the sample deformation under both CP and AC. Fig. 9 illustrates the model restriction to clearly show the sample deformation.

Fig. 9. Model Restriction

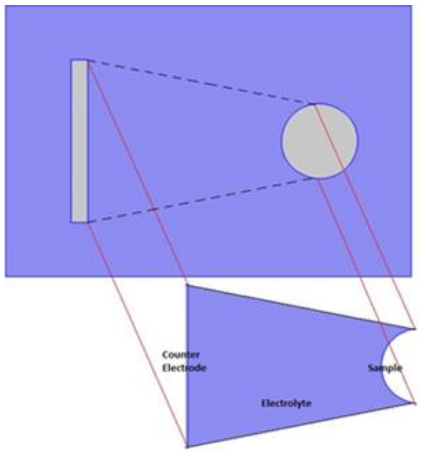

Fig. 10 shows that corrosion made a clear sample deformation when subjected to both CP and an induced AC, and when we applied our immunity program (Fig.11) during the same period (72 hours), we did not observe any deformation.

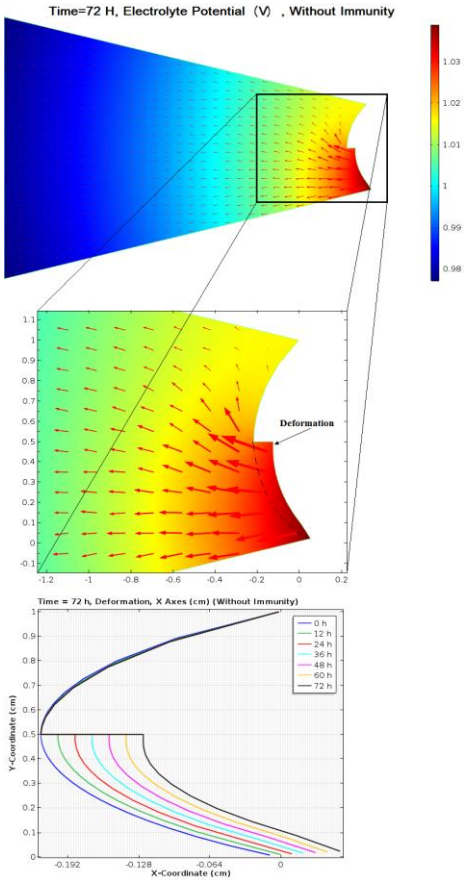

Fig. 10. Sample Deformation by corrosion (under CP and AC)

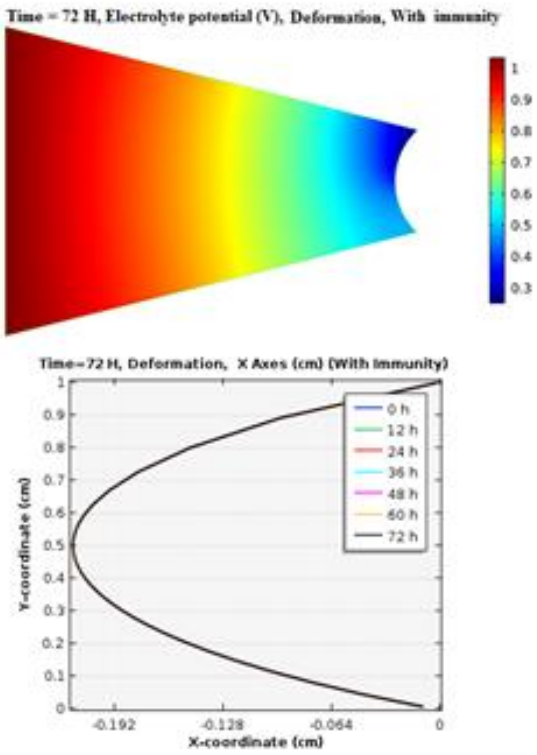

Fig. 11. The Deformation State after the implementation of the program to return to the immunity zone.

1.5 Comparison between experimental and simulation results

To clarify the motivation for the present research, we would like to provide the direct links between the experimental and simulation study. We have used the same steel API5L X52 in the experiment and the one that was configured in the simulation. The potential Φ_s applied to the studied sample in the experimental part obeyed to the formula eq. (5), which is the same used in the numerical simulation eq. (7).

Figs. 12 and 13 Show that the experimental results are in agreement with simulation results.

These results are also fully compatible with the standards of the Iron Pourbais and Hosokawa diagrams [1][2][4].

The execution of the corrective program of CP if the E_{off} exceeds the limits is possible in the simulation, but experimentally it is not possible by the used device potentiostat.

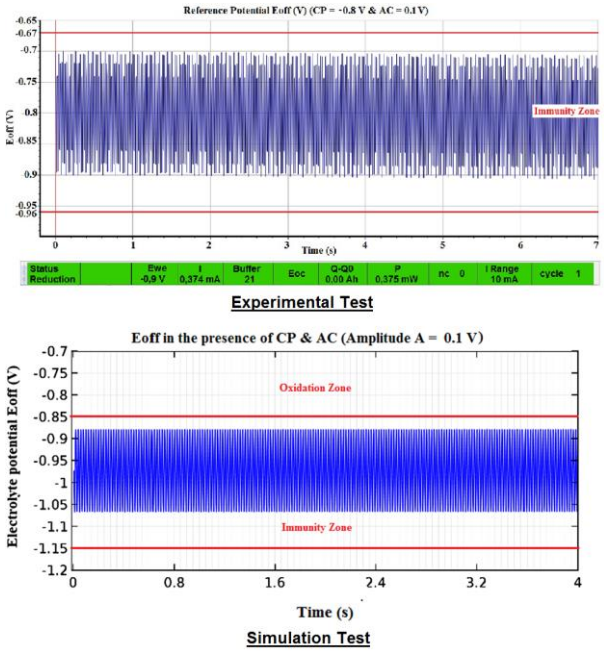

Fig. 12. Comparison between experimental result in Fig. 4 and simulation results in Fig. 6.

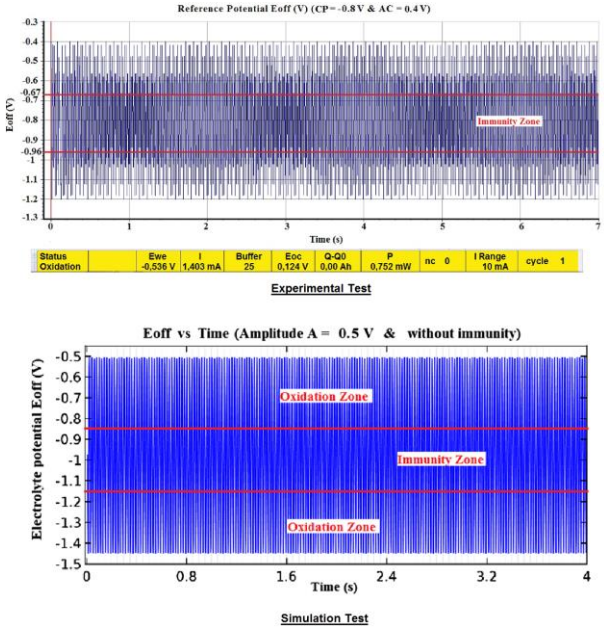

Fig. 13. Comparison between experimental result in Fig. 5 and simulation results in Fig. 7.

Conclusion

In conclusion, in the practical study we were able to model the AC corrosion phenomena. And it allowed us, first, to record data such as the free potential, it showed that without the CP the sample was in oxidation state. Secondly, we have selected the proper CP in the absence of AC, by applying the LP analysis method (Linear Polarization: Log i (E_{off})) on two different samples, results illustrated that for an adequate CP chosen in reduction area the sample does not undergo any corrosion, it was in the immunity zone, these tests results are consistent with the standards. Finally, the application of AC to a model protected by a CP, for low AC

voltage, gave no oxidation because we did not exceed the immunity zone, and the sample was safe, but when AC increased, E_{off} exceeded the immunity area, and the oxidation took place. Regarding the numerical simulation, the results indicated that the induced AC caused the corrosion of the sample, which was cathodically protected because we found an E_{off} exceeding the immunity zone and a strong iron oxidation. We have also simulated the oxygen and the hydrogen concentration in the electrolyte, and the sample deformation. Then, using our monitoring program has allowed us to bring the E_{off}, in the AC presence, in corrosion immunity zone according to standards, to minimise the electrochemical process reactions and it equally prevents the sample's deformation.

The direct links between the experimental and simulation study are that we have used the same steel (API 5L X52) and the potential applied to the studied sample obeyed to the same formula, it was equal to the addition of a direct value as a CP and an alternating value as AC interference (eq. (5) and eq. (7)); results have shown that the experimental data are in agreement with simulation ones; the execution of the CP monitoring and corrective program in case that the E_{off} exceeds the limits is possible in the simulation, but experimentally it is not possible by the used device, the potentiostat and galvanostat.

To sum up, in our future perspective, our goal is to establish a system provided with a microcontroller to monitor the CP and for implementing the immunity program in addition to the existing CP system in places where pipelines are near power lines and causing AC interferences.

Acknowledgment

We would like to thank Laboratory of Process Engineering Department and Laboratory of Mechanics, Amar Telidji University of Laghouat, Algeria, for providing us with the potentiostat and galvanostat VoltaLab PGZ402 and EC-LAB SP150 and ENS (Higher Normal School of Laghouat) for EC-LAB VSP300. The authors thank Professor M. Madjid TEGUAR, Research Laboratory of Electrical Engineering, National Polytechnic Ecol, B.P 182, El-Harrach, Algeria for Comsol code.

References

[1] Brenna A, Lazzari L, Castiglioni C. A proposal of AC corrosion mechanism of carbon steel in cathodic protection condition. PhD, Thesis. Materials Engin, Polytechnic, Milano Italy; 2012.

[2] Hosokawa Y, Kajiyama F, Nakamura Y. New cathodic protection criteria based on direct and alternating current densities measured using coupons and their application to modern steel pipelines. J. Corrosion 2004; 60(3):304-312.

[3] Nielsen LV, Nielsen KV, Baumgarten B, Breuning-Madsen H, Cohn P, Rosenberg H. AC induced corrosion in pipelines: detection, characterization and mitigation. Int. Conf. Corrosion 2004. NACE.

[4] Hosokawa Y, Kajiyama F, Nakamura Y. Overcoming the new threat to pipeline integrity-AC corrosion assessment and its mitigation. Int. 23rd World Gas Conference 2006, Amsterdam Netherlands.

[5] Qingmiao D, Yueming F. Experimental Study on the Influence of AC Stray Current on the Cathodic Protection of Buried Pipe. Intern. J. of Corrosion 2016, Art. Id.561392.

[6] BV C, OY C. COMSOL Multiphysics User's Guide©. Comsol AB, Comsol ed, 2010.

[7] Nichols P, Holtsbaum B, Mayfield D, Nelson S, Parker K. CP3-Cathodic Protection. Tech. C. Manual, Houston, NACE ed: 2008.

[8] Hosokawa Y, Kajiyama F, Nakamura Y. New CP criteria for elimination of the risks of AC corrosion and overprotection on cathodically protected pipelines. Corrosion 2002, NACE, Denver, CO, USA, 2002, paper 02111.

[9] Wakelin G, Gummow RA, Segall SM. AC corrosion - Case histories test procedures and mitigation. Corrosion/98, NACE Int. San Diego, CA, USA, 1998, paper 98565.

[10] BioLogic. EC-Lab Software: Techniques and Applications. V. 10.1x., February, BioiLogic Science Instruments ed; 2011.

[11] Kofstad P, Norby T. Defects and Transport in crystalline solids. Department of Chemistry, University of OSLO; Sept. 2007.

[12] Muehlenkamp E, Koretsky M. Effect of moisture on the spatial uniformity of cathodic protection of steel in reinforced concrete. J. Corrosion, 2005; 61(6):519-533.